Talanta 130 (2014) 259–264

Contents lists available at ScienceDirect

Talanta

journal homepage: www.elsevier.com/locate/talanta

Fe_3O_4 peroxidase mimetics as a general strategy for the fluorescent detection of H_2O_2-involved systems

Yun Shi, Ping Su, Yingying Wang, Yi Yang*

College of Science, Beijing Key Laboratory of Environmentally Harmful Chemical Analysis, Beijing University of Chemical Technology, Beijing 100029, PR China

ARTICLE INFO

Article history:
Received 29 April 2014
Received in revised form
19 June 2014
Accepted 22 June 2014
Available online 3 July 2014

Keywords:
Fe_3O_4 magnetic microsphere
Peroxidase mimetic
General system
Hydrogen peroxide
Glucose
p-Nitrophenol

ABSTRACT

Enzyme mimetics have recently attracted considerable interest because of their high stability and low cost. We developed a general H_2O_2-involved fluorescence system using Fe_3O_4 magnetic microspheres as peroxidase mimetics and benzoic acid (BA) as indicator. Glucose and p-nitrophenol were used as models to determine the characteristics and effectiveness of the system. Glucose oxidase hydrolyzes glucose, in the presence of oxygen, to H_2O_2 followed by the activation of Fe_3O_4 MMs, resulting in the catalyzed oxidation of benzoic acid. Glucose can be determined by the quantitative fluorescence production. p-Nitrophenol is determined as model compounds which competes with benzoic acid for H_2O_2 resulting in the decreased catalytic oxidation of benzoic acid with the Fe_3O_4 MMs. The detection limit of the Fe_3O_4/H_2O_2/BA system is 0.008 μM for H_2O_2, 0.025 μM for glucose and 0.05 μM for p-nitrophenol. Furthermore, the system had high sensitivity, good selectivity and was capable of sensing glucose in human serum and p-nitrophenol in water samples. The proposed system has great potential in the chemical/biological sensing of a variety of analytes associated with reactions that produce or consume H_2O_2.

1. Introduction

Natural enzymes are of widespread interest because of their intrinsic catalytic activity and high substrate specificity under mild conditions. However, the practical application of enzymes is often hampered by intrinsic drawbacks such as the sensitivity of catalytic activity toward environmental conditions, inherent instability because of denaturation, and their expensive preparation and purification [1]. Recently, mimetic enzymes that can be used as enzyme substitutes have received extensive attention because of their controlled synthesis, low cost, tunable catalytic activities, and high degree of stability under stringent conditions. Fe_3O_4 magnetic microspheres (Fe_3O_4 MMs) [2,3], nanoceria [4], C_{60} [5], graphene dots [6], and other nanoparticles [7–9] have been evaluated as mimetic enzymes and have been found to possess high catalytic activities. Fe_3O_4 MMs as highly efficient peroxidase mimetics are apparently superior because they retain their activity over a wide range of pH and temperatures. Their syntheses are characterized by high yields at comparatively low cost and easy separation.

Recently, Gao et al. [2] reported that Fe_3O_4 MMs exhibit peroxidase activity allowing the effective determination of hydrogen peroxide (H_2O_2). Since then, peroxidase mimetics-based methods for H_2O_2 have been evaluated by spectrophotometry [2,10], amperometry [11] and chemiluminescence [12,13]. Fluorescence is highly sensitive and selective and has a fast response and simple operation but it has rarely been used for H_2O_2 detection because of unsuitable fluorescence indicators. Benzoic acid (BA), as a fluorescence indicator, can be slowly oxidized by H_2O_2 but it is highly reactive in the presence of OH· derived from Fe_3O_4 MMs and H_2O_2 to produce hydroxybenzoic acid (OHBA) with strong fluorescence [14]. This encouraged us to fabricate general fluorescence chemosensors based on the Fe_3O_4/H_2O_2/BA system for the detection of target compounds that generate or consume H_2O_2 with glucose and p-nitrophenol (PNP) as examples, respectively.

Glucose has a well-known direct association with diabetes and it produces H_2O_2 in the presence of glucose oxidase (GOx), hence much effort has been put into the development of glucose sensors [15,16]. Most conventional glucose sensors rely on enzymatically based sensing [16,17] and the fluorescence-based detection of glucose is relatively rare [3,18]. PNP is a carcinogenic substituted phenol and is considered a hazardous waste and a priority toxic pollutant [19]. PNP consumes H_2O_2 when coupled with Fe_3O_4 and this enables the degradation of high concentrations of PNP with

Abbreviations: MMs, magnetic microspheres; BA, benzoic acid; OHBA, hydroxybenzoic acid; PNP, p-nitrophenol; GOx, glucose oxidase

* Corresponding author. Tel./fax: +86 10 64434898.
E-mail address: yangyi@mail.buct.edu.cn (Y. Yang).

http://dx.doi.org/10.1016/j.talanta.2014.06.053
0039-9140/

operational convenience, simple instruments, and low cost [20,21]. However, this method cannot be used to quantify PNP at low concentrations because of poor response signals and interference by impurities. Therefore, the introduction of a PNP system with significant response is essential.

Herein, we present Fe_3O_4 MMs peroxidase mimetic-based fluorescence analysis for the detection of glucose and PNP as these are analytes that represent the generation and consumption of H_2O_2, respectively. The novel fluorescence biosensors were successfully applied to the determination of glucose in human serum samples, and PNP in water samples using simple procedures with high sensitivity and selectivity.

2. Experimental

2.1. Materials

GOx (EC 1.1.3.4 from Aspergillus niger, 109 U/mg) was obtained from Amresco (Solon, OH, USA). Glucose was purchased from TCI (Tokyo, Japan). p-Nitrophenol was obtained from AccuStandard (New Haven, CT, USA). Galactose was purchased from Alfa Aesar Co. Ltd. (Dora, FL, USA). Hydrogen peroxide (H_2O_2, 30%), benzoic acid, ferric chloride hexahydrate ($FeCl_3 \cdot 6H_2O$), sucrose, maltose and fructose were supplied by Beijing Yili Chemical (Beijing, China). All other chemical reagents used in the experiments were of analytical grade.

The fluorescence signals of the system were all recorded on an F-7000 fluorescence spectrophotometer (Hitachi, Japan). The sizes and morphologies of the Fe_3O_4 MMs were determined using a transmission electron microscope (TEM, Hitachi H800, Tokyo, Japan).

2.2. Preparation of the Fe_3O_4 MMs

The Fe_3O_4 MMs were synthesized by a solvothermal reaction as previously described [22]. Briefly, 1.35 g $FeCl_3$•$6H_2O$ and 3.6 g sodium acetate were dissolved in 40 mL ethylene glycol under vigorous stirring for 30 min. The mixture was sealed in a polytetrafluoroethylene-lined stainless steel autoclave and heated at 200 °C for 8 h. The black Fe_3O_4 MMs that formed were separated using a magnet and further washed with ethanol three times before drying under vacuum at 50 °C for 5 h.

2.3. H_2O_2 detection with the Fe_3O_4 MMs

The reaction conditions for the determination of H_2O_2 were as follows: Fe_3O_4 MMs were first mixed with H_2O_2 in 5 mL phosphate buffer (50 mM, pH 3.0) using BA as the fluorescent indicator. After incubation at room temperature, the pH of the resultant hydroxybenzoic acid solution was adjusted to pH 11.0 using 1 M NaOH to stop the reaction and improve the fluorescence behavior. The Fe_3O_4 MMs were isolated from the resulting solution by an external magnetic field. The supernatant was filtered using a 0.45-μm filter and investigated using the fluorescence spectrophotometer. Water of the same volume was used instead of H_2O_2 and the ΔF was determined where $\Delta F = F(H_2O_2, 405\ nm) - F(blank, 405\ nm)$. Moreover, the optimal reaction conditions for the Fe_3O_4/H_2O_2/BA system were used for the determination of H_2O_2 at different concentrations according to the procedure above. The experiment was repeated three times, and the average fluorescence signal was obtained.

2.4. Glucose detection using the Fe_3O_4 MMs

Glucose detection was realized as follows: 100 μL of 1 mg mL^{-1} GOx was incubated with various concentrations of glucose (or diluted serum sample) in 4.25 mL of phosphate buffer (50 mM, pH 7.0) for 30 min at room temperature. Thereafter, 50 μL of 100 mg ml^{-1} Fe_3O_4 MMs and 500 μL of 14 mM BA were added to the above-mentioned solution and reacted for another 30 min at room temperature. 1 M NaOH was then used to terminate the reaction. Finally, the solution without the Fe_3O_4 MMs was used to compile a standard curve. Water of the same volume was used instead of glucose and the ΔF was determined where $\Delta F = F(glucose, 405\ nm) - F(blank, 405\ nm)$. To study the specificity of the proposed Fe_3O_4/H_2O_2/BA system toward glucose, 1 mM of galactose, maltose, lactose and fructose were used instead of 1 mM glucose.

2.5. PNP detection using the Fe_3O_4 MMs

The PNP samples were analyzed as follows: 50 μL of 100 mg ml^{-1} Fe_3O_4 MMs, 50 μL of 0.8 mM H_2O_2 and 50 μL with different concentrations of PNP (or a water sample) were added to 4.35 mL phosphate buffer (50 mM, pH 3.0). The measurement started upon the addition of 500 μL of 14 mM BA, which was allowed to react for 30 min at room temperature. Water of the same volume was used instead of PNP and the ΔF was determined where $\Delta F = F(blank, 405\ nm) - F(PNP, 405\ nm)$.

3. Results and discussion

3.1. Characterization of the Fe_3O_4 MMs

The size and morphology of the synthesized Fe_3O_4 MMs were observed by TEM and the mean diameter was determined to be approximately 350 nm (Fig. S1).

3.2. Detection method

We used an Fe_3O_4 MMs peroxidase mimetic-based fluorescence assay to detect glucose and PNP. As shown in Scheme 1A, GOx hydrolyzes glucose to produce H_2O_2, which activates the Fe_3O_4 MMs and catalyzes the oxidation of BA to produce a strongly fluorescent product OHBA quantitatively, and this can be monitored by fluorescence spectrophotometry. PNP consumes H_2O_2 upon catalysis by the Fe_3O_4 MMs and the reaction between BA and H_2O_2 weakens, leading to a decrease in the amount of the strongly fluorescent product OHBA. Therefore, different concentrations of PNP can be determined (Scheme 1B).

3.3. Peroxidase mimetic catalytic activity of the Fe_3O_4 MMs

To investigate the peroxidase mimetic catalytic activity of the Fe_3O_4 MMs, a Fe_3O_4 MMs-catalyzed reaction between the

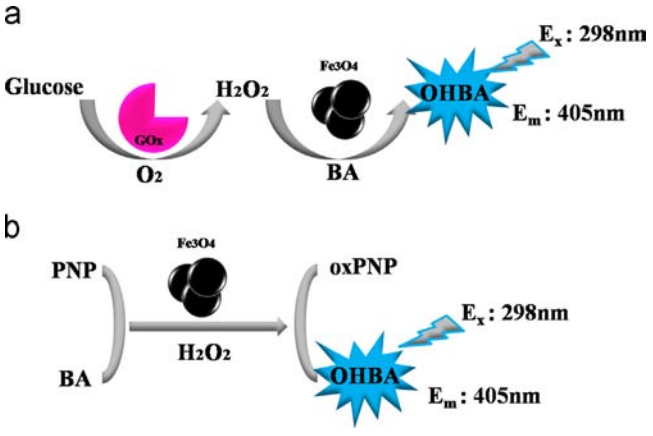

Scheme 1. Schematic diagram of (A) glucose detection using Fe_3O_4/H_2O_2/BA system and (B) PNP detection using Fe_3O_4/H_2O_2/BA system.

fluorescent indicator BA and H_2O_2 was evaluated. As shown in Fig. S2, the oxidation product of BA has a characteristic emission peak at 405 nm when excited at 298 nm [18]. BA (Fig. 1a) and a mixture of BA with either Fe_3O_4 (Fig. 1b) or H_2O_2 (Fig. 1c) is weakly fluorescent but the resulting solution of Fe_3O_4, H_2O_2 and BA is strongly fluorescent (Fig. 1d). The fluorescence intensity was approximately 35 times that in the absence of the Fe_3O_4 MMs. These phenomena indicate that the Fe_3O_4 MMs possess highly efficient peroxidase mimetic catalytic activity in the Fe_3O_4/H_2O_2/BA system, which is required to measure H_2O_2.

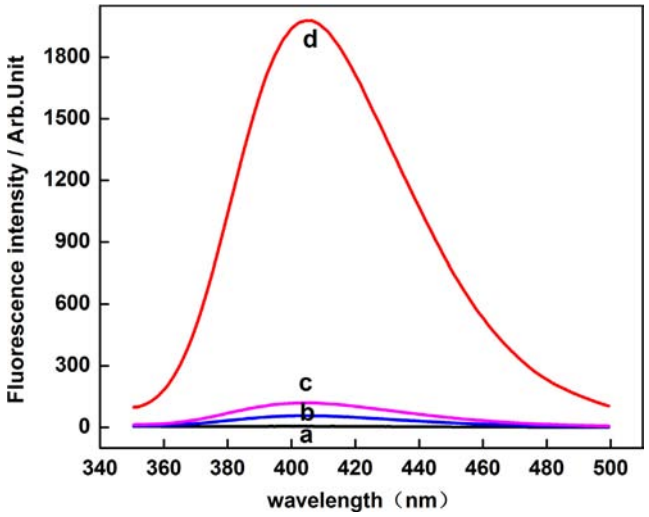

Fig. 1. The fluorescence changes of the system under different conditions are as follows: (a) BA (1.0 mmol L^{-1}); (b) BA (1.0 mmol L^{-1})+Fe_3O_4 (1.6 g L^{-1}); (c) BA (1.0 mmol L^{-1})+H_2O_2 (16.0×10^{-6} mol L^{-1}); and (d) BA (1.0 mmol L^{-1})+Fe_3O_4 (1.6 g L^{-1})+H_2O_2 (16.0×10^{-6} mol L^{-1}).

To optimize the analytical method for the determination of H_2O_2, the effects of experimental conditions including pH, reaction time, Fe_3O_4 MMs concentration, and BA concentration were investigated. As shown in Fig. 2A, the catalytic activity initially increased with an increase in pH up to 3.0 and it is because the surplus hydrogen ions favor a backward reaction leading to an increase in the Fe(III) concentration [23]. The catalytic activity decreased as the pH was continue to increased owing to the deactivation of ferrous [23] and the optimum pH was thus 3.0. The effect of incubation time on the catalytic efficiency of the Fe_3O_4 MMs is shown in Fig. 2B. A longer incubation time allows the substrate to react more completely with H_2O_2 but it does increase the duration of the experiments. The optimum incubation time of 30 min was used for subsequent experiments. The effect of Fe_3O_4 MMs concentration on reaction activity was determined between 0.2 g L^{-1} and 1.6 g L^{-1}, and the optimum was found to be 1.0 g L^{-1} (Fig. 2C). Additionally, the fluorescence value initially tended to increase with an increase in BA concentration up to 1.4 mmol L^{-1}, but further increases in concentration did not increase the

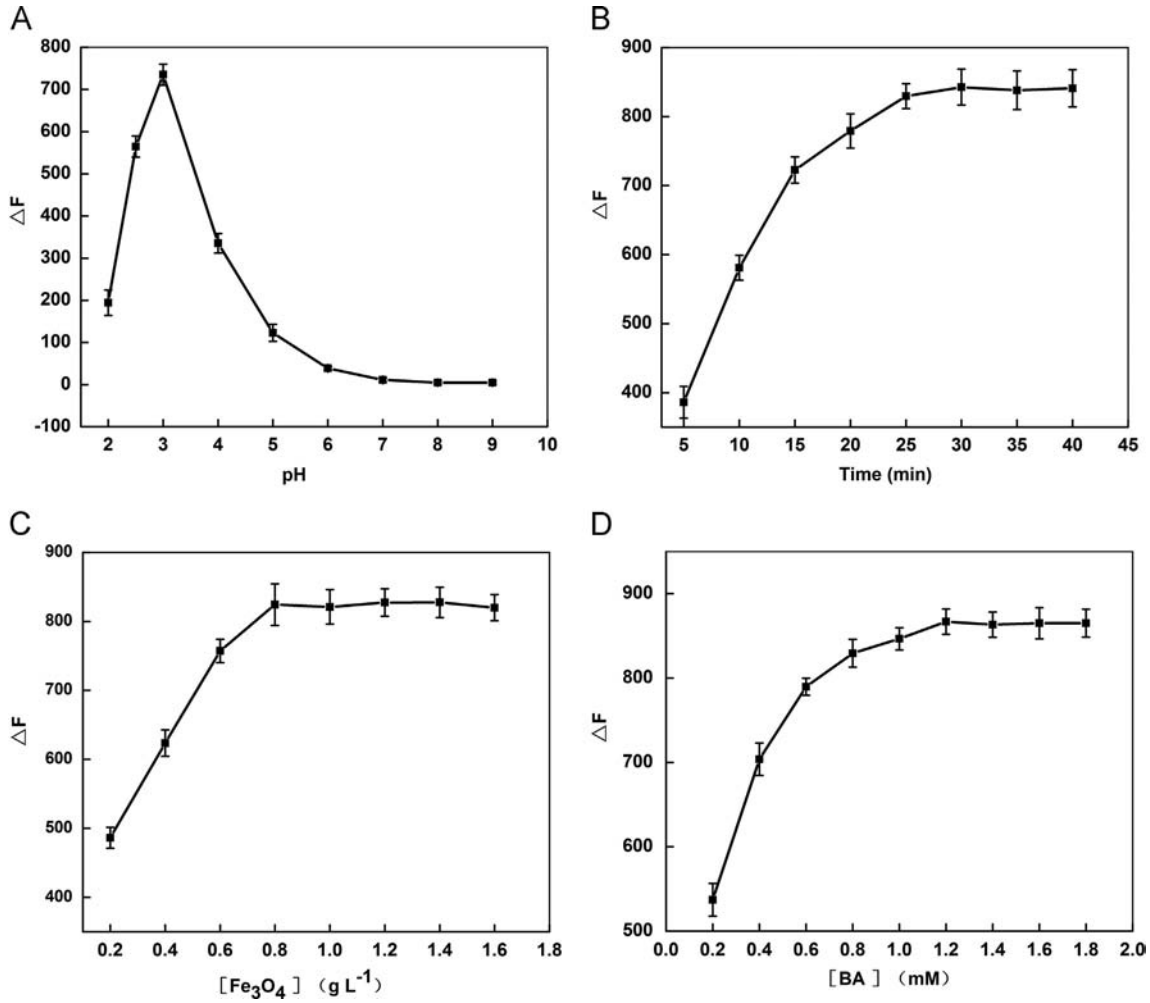

Fig. 2. Optimization of following catalytic conditions: (A) effect of pH on the fluorescence intensity; (B) effect of reaction time on the fluorescence intensity; (C) effect of Fe_3O_4 MMs concentration on the fluorescence intensity; and (D) effect of BA concentration on the fluorescence intensity. Catalytic conditions $-\Delta F$ curve for H_2O_2 detection where $\Delta F = F(H_2O_2, 405\text{ nm}) - F(\text{blank}, 405\text{ nm})$. The error bars represent the standard deviation of three measurements.

catalytic efficiency significantly because of the apparent saturation of fluorescence intensity, which is attributed to a complete reduction of H_2O_2 in the reaction system (Fig. 2D).

3.4. H_2O_2 detection using Fe_3O_4 as a peroxidase mimetic

The catalytic activity of Fe_3O_4 MMs is H_2O_2 concentration dependent. A calibration curve of H_2O_2 sensing under optimal conditions (i.e., pH=3.0, 30 min, 1.0 g L^{-1} Fe_3O_4 MMs, 1.4 mmol L^{-1} BA) was compiled. As shown in Fig. 3, a prominent increase in the fluorescence intensity was observed as the concentration of H_2O_2 increased from 0.04 μM to 20 μM. The inset in Fig. 3 shows a typical H_2O_2 concentration–response curve where it has a linear range between 0.04 μM and 8.0 μM. Detection limit was detected by diluting with sample solution basing on 3S/N. It was found in the experiment that the detection limit of H_2O_2 was 0.008 μM, which was much lower than that of other nanomaterial-catalyzed methods [2,3,5,7–9,24–27].

3.5. Glucose detection using Fe_3O_4 as a peroxidase mimetic

3.5.1. Calibration curve for glucose detection

H_2O_2 is the main product of glucose oxidation by GOx in the presence of oxygen. Consequently, glucose detection can be realized by coupling Fe_3O_4 MMs-based catalytic methods with GOx-based glucose oxidation, which illustrates the feasibility of the universal Fe_3O_4/H_2O_2/BA system upon the generation of H_2O_2. Because of the denaturation of GOx at pH 3.0, glucose detection was performed in two separate steps as mentioned in the experimental section. After the completion of the enzymatic hydrolysis reaction in a pH 7.0 buffer solution, the H_2O_2 produced by glucose oxidation with GOx was determined using the Fe_3O_4 MMs. In this way, a fluorometric method for the determination of glucose was easily realized in this work. Fig. 4 shows a typical glucose concentration-response curve, suggesting that this method has a linear range between 0.05 μM and 10 μM with a low detection limit of 0.025 μM, which is much lower than that usually used for glucose [6,9,15,26–30].

3.5.2. Selectivity during glucose detection

We further examined the specificity of the proposed Fe_3O_4-based system toward glucose detection, and the experiments were performed under the same conditions using saccharides such as fructose, galactose, sucrose and maltose. To determine the discrimination ability of this method, the distinction factor (DF) was determined as $(F_2-F_0)/(F_1-F_0)$, where F_1, F_2 and F_0 are the fluorescence intensities found for glucose, the other sugars and the background, respectively. As shown in Fig. 5, this system is highly sensitive and selective toward glucose but had a poor response toward the other saccharides even at control sample concentrations as high as 1 mM. As a result, high specificity is guaranteed in this system.

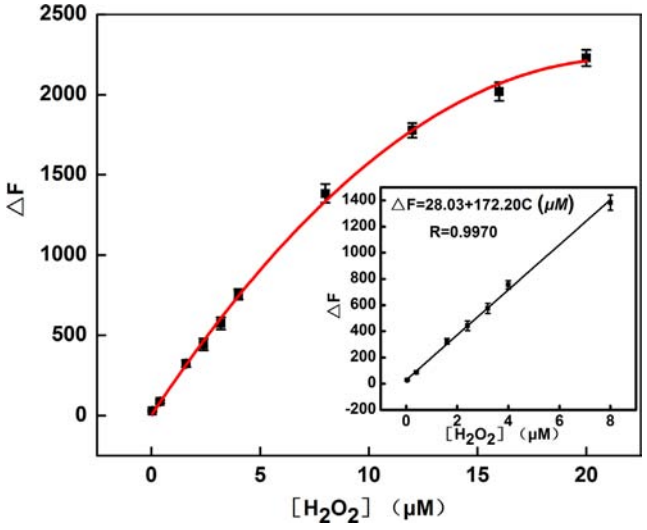

Fig. 3. Calibration curve of the H_2O_2 sensing. The inset gives the linear correlation between the ΔF and H_2O_2 concentration, where $\Delta F=F(H_2O_2, 405\ nm)-F(blank, 405\ nm)$ ($N=3$). Reaction conditions: 1.0 g L^{-1} Fe_3O_4 MMs, 1.4 mmol L^{-1} BA, pH 3.0, and reaction time 30 min.

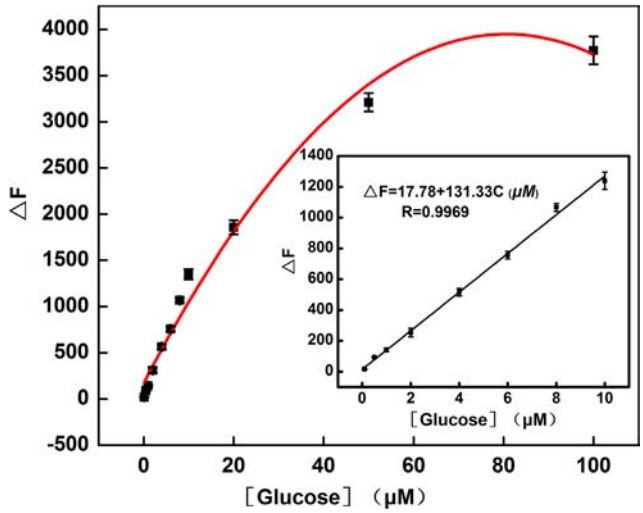

Fig. 4. Calibration curve of the glucose sensing. The inset gives the linear correlation between the ΔF and glucose concentration, where $\Delta F=F$(glucose, 405 nm) − F(blank, 405 nm) ($N=3$).

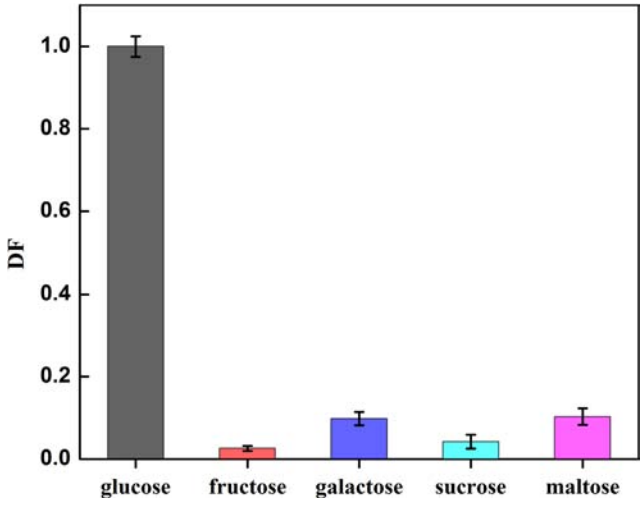

Fig. 5. The signal difference between glucose and other sugars (fructose, galactose, sucrose and maltose, each at 1 mM) ($N=3$).

3.5.3. Detection of glucose in serum samples

The feasibility of the assay for the detection of glucose was verified by the analysis of real human blood serum samples. The serum samples were diluted 1000 times to eliminate any possible complex matrix effects and to ensure that the concentration of glucose in the samples was within the linear range of the calibration curve. Excellent agreement exists between the proposed method and the classic glucose meter method (Table 1). Moreover, when 4 mM glucose was added to the serum samples,

Table 1
Determination of glucose in healthy human serum samples ($n=3$).

Sample	Glucose concentration (mmol L^{-1})		Relative error (%)	Glucose add (mmol L^{-1})	Recovery (%)
	Hospital method[a]	BA method[b]			
1	4.10	4.32 ± 0.29	5.36	4	102.10
2	4.70	4.58 ± 0.22	2.55	4	98.62
3	5.20	5.35 ± 0.17	2.88	4	97.72

[a] Results obtained by the Hospital of Beijing University of People's Hospital.
[b] Results obtained by this work.

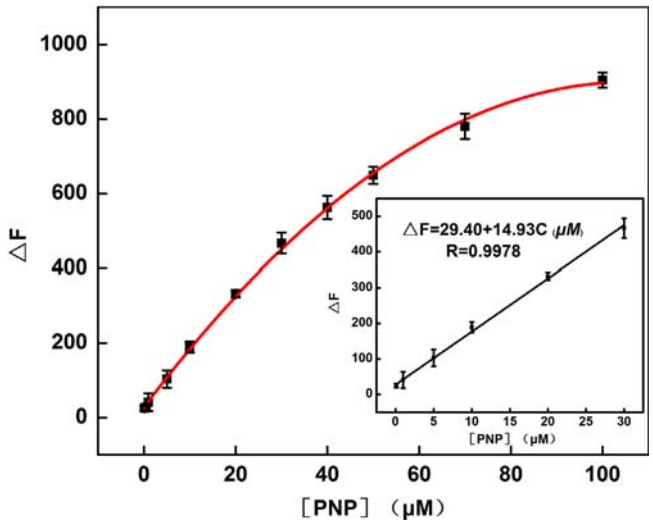

Fig. 6. Calibration curve of the PNP sensing. The inset gives the linear correlation between the ΔF and PNP concentration, where $\Delta F = F$(blank, 405 nm) $- F$(PNP, 405 nm) ($N=3$).

the recovery of glucose varied within a range of 96.1–102.1%, which shows that the proposed method is suitable for glucose detection in a serum sample.

3.6. PNP detection using Fe_3O_4 as a peroxidase mimetic

3.6.1. Calibration curve for PNP detection

The Fe_3O_4/H_2O_2/BA system was used to detect PNP by monitoring the consumption of H_2O_2 at pH 3.0, which exploits the competition between BA and PNP for H_2O_2. Thus, the concentration of H_2O_2 may have a large influence on the PNP detection system. Considering the moderate catalytic rate of Fe_3O_4 MMs, we chose 8 μM as the H_2O_2 reaction concentration to ensure that it was within the linear range and that it was sensitive enough for the proposed method. Fig. 6 shows a typical PNP concentration–response curve, which indicates that this method has a linear response range from 0.1 μM to 30 μM with a fairly low detection limit of 0.05 μM compared with other methods [19,31,32]. Hence, the fluorescence sensor based on Fe_3O_4 MMs is adequate for the detection of PNP concentration because of the simple process, its sensitivity, and its low cost.

3.6.2. Detection of PNP in water samples

The proposed method was used to analyze PNP in real water samples (tap water and water from the Yuandadu river), and no response corresponding to PNP was observed. Different quantities of PNP were added to the samples. As is shown in Table 2, the concentrations of PNP in the spiked water samples determined by the proposed method were in good agreement with those of PNP added. Quantitative recoveries of both ranged from 94.70% to 96.60% and from 94.40% to 95.98%, respectively, which showed that the fluorescence sensor based on Fe_3O_4/H_2O_2/BA can potentially be used for PNP detection in real samples.

Table 2
Determination of PNP in water ($n=3$).

Sample	Add (μmol L^{-1})	Found (μmol L^{-1})	RSD (%)	Recovery (%)
Tap water	0	ND[a]	1.07	–
	5	4.83	2.91	96.60
	10	9.47	3.23	94.70
	20	19.02	2.85	95.12
Yuandadu river	0	ND	2.03	–
	5	4.72	3.58	94.40
	10	9.51	2.45	95.10
	20	19.19	2.98	95.98

[a] ND: not detected.

4. Conclusion

We show the viability of using an Fe_3O_4 MMs peroxidase mimetic-based fluorescence assay for the detection of glucose and PNP. Because of its high catalytic activity, the Fe_3O_4 MMs-based system permits detection of as low as 0.008 μM H_2O_2, which is much lower than that of other nanomaterial-catalyzed methods. The detection limit was found to be 0.025 μM for glucose and 0.05 μM for PNP. Furthermore, the application of the developed method to the determination of glucose in a human serum sample and to the determination of PNP in tap water and in the Yuandadu river were evaluated and satisfactory results were obtained. The Fe_3O_4/H_2O_2/BA system thus has many advantages including high sensitivity and selectivity, simple operation, and low cost. This can potentially realize accurate quantitative analysis in biomedical diagnoses and can be used for the environmental monitoring of species associated with H_2O_2.

Acknowledgments

This study was supported by the National Natural Science Foundation of China (No. 21075008), and Beijing Natural Science Foundation (No. 2132048).

Appendix A. Supporting information

Supplementary data associated with this article can be found in the online version at http://dx.doi.org/10.1016/j.talanta.2014.06.053.

References

[1] Y. Lin, J. Ren, X. Qu, Acc. Chem. Res. 47 (2014) 1097–1105.
[2] L. Gao, J. Zhuang, L. Nie, J. Zhang, Y. Zhang, N. Gu, T. Wang, J. Feng, D. Yang, S. Perrett, X. Yan, Nat. Nanotechnol. 2 (2007) 577–583.
[3] Y. Gao, G. Wang, H. Huang, J. Hu, S.M. Shah, X. Su, Talanta 85 (2011) 1075–1080.
[4] A. Hayat, S. Andreescu, Anal. Chem. 85 (2013) 10028–10032.
[5] R. Li, M. Zhen, M. Guan, D. Chen, G. Zhang, J. Ge, P. Gong, C. Wang, C. Shu, Biosens. Bioelectron. 47 (2013) 502–507.
[6] A.X. Zheng, Z.X. Cong, J.R. Wang, J. Li, H.H. Yang, G.N. Chen, Biosens. Bioelectron. 49 (2013) 519–524.
[7] A.K. Dutta, S. Das, S. Samanta, P.K. Samanta, B. Adhikary, P. Biswas, Talanta 107 (2013) 361–367.
[8] W. Zhang, D. Ma, J. Du, Talanta 120 (2014) 362–367.
[9] M. Liu, B. Li, X. Cui, Talanta 115 (2013) 837–841.
[10] H. Wei, E.k. Wang, Anal. Chem. 80 (2008) 2250–2254.

[11] T.C. Nagaiah, D. Schafer, W. Schuhmann, N. Dimcheva, Anal. Chem. 85 (2013) 7897–7903.
[12] Z. Wang, F. Liu, C. Lu, Biosens. Bioelectron. 38 (2012) 284–288.
[13] W. Shi, X. Zhang, S. He, Y. Huang, Chem. Commun. 47 (2011) 10785–10787.
[14] S.S. Chou, C.P. Huang, Chemosphere 38 (1999) 2719–2731.
[15] J. Xie, H. Cao, H. Jiang, Y. Chen, W. Shi, H. Zheng, Y. Huang, Anal. Chim. Acta 796 (2013) 92–100.
[16] D.Y. Zhai, B.R. Liu, Y. Shi, L.J. Pan, Y.Q. Wang, W.B. Li, R. Zhang, G.H. Yu, ACS Nano 7 (2013) 3540–3546.
[17] S. Tierney, B.M.H. Falch, D.R. Hjelme, B.T. Stokke, Anal. Chem. 81 (2009) 3630–3636.
[18] W. Luo, Y.S. Li, J. Yuan, L. Zhu, Z. Liu, H. Tang, S. Liu, Talanta 81 (2010) 901–907.
[19] J. Li, D. Kuang, Y. Feng, F. Zhang, Z. Xu, M. Liu, J. Hazard. Mater. 201–202 (2012) 250–259.
[20] A.A. Pradhan, P.R. Gogate, J. Hazard. Mater. 173 (2010) 517–522.
[21] J.A. Banuelos, F.J. Rodriguez, J. Manriquez Rocha, E. Bustos, A. Rodriguez, J.C. Cruz, L.G. Arriaga, L.A. Godinez, Environ. Sci. Technol. 47 (2013) 7927–7933.
[22] H. Deng, X.L. Li, Q. Peng, X. Wang, J.P. Chen, Y.D. Li, Angew. Chem. 117 (2005) 2842–2845.
[23] N.N. Wang, T. Zheng, J.P. Jiang, W.S. Lung, X.J. Miao, P. Wang, Chem. Eng. J. 239 (2014) 351–359.
[24] S. Guo, D. Wen, S. Dong, E.K. Wang, Talanta 77 (2009) 1510–1517.
[25] S. He, W. Shi, X. Zhang, J. Li, Y. Huang, Talanta 82 (2010) 377–383.
[26] L. Hu, Y. Yuan, L. Zhang, J. Zhao, S. Majeed, G. Xu, Anal. Chim. Acta 762 (2013) 83–86.
[27] N. Li, Y. Yan, B.Y. Xia, J.Y. Wang, X. Wang, Biosens. Bioelectron. 54 (2014) 521–527.
[28] S. Ci, T. Huang, Z. Wen, S. Cui, S. Mao, D.A. Steeber, J. Chen, Biosens. Bioelectron. 54 (2014) 251–257.
[29] R.M. Li, M.M. Zhen, M.R. Guan, D.Q. Chen, G.Q. Zhang, J.C. Ge, P. Gong, C.R. Wang, C.Y. Shu, Biosens. Bioelectron. 47 (2013) 502–507.
[30] Z. Xing, J. Tian, A.M. Asiri, A.H. Qusti, A.O. Al-Youbi, X. Sun, Biosens. Bioelectron. 52 (2014) 452–457.
[31] J.X. Liu, H. Chen, Z. Lin, J.M. Lin, Anal. Chem. 82 (2010) 7380–7386.
[32] Y. Zhou, Z.B. Qu, Y. Zeng, T. Zhou, G. Shi, Biosens. Bioelectron. 52 (2014) 317–323.